NUMERICAL SIMULATIONS OF DEGENERATE TRANSPORT PROBLEMS

FLORIAN DE VUYST AND FRANCESCO SALVARANI

ABSTRACT. We consider in this article the monokinetic linear Boltzmann equation in two space dimensions with degenerate cross section and produce, by means of a finite-volume method, numerical simulations of the large-time asymptotics of the solution.

The numerical computations are performed in the $2Dx - 1Dv$ phase space on Cartesian grids and deal with both cross sections satisfying the geometrical condition and cross sections that do not satisfy it.

The numerical simulations confirm the theoretical results on the long-time behaviour of degenerate kinetic equations for cross sections satisfying the geometrical condition. Moreover, they suggest that, for general non-trivial degenerate cross sections whose support contains a ball, the theoretical upper bound of order $t^{-1/2}$ for the time decay rate (in L^2-sense) can actually be reached.

1. INTRODUCTION

This paper aims to give some numerical experiments in order to clarify an open question concerning the mathematical theory of the linear Boltzmann equation.

The linear Boltzmann equation is a model, whose explicit form will be presented in the next section, that describes at the simplest possible level the dynamics of an ensemble of particles (for example, neutrons or photons) at the mesoscopic scale, by taking into account the effects of an host medium on the particle population. The interactions between particles and medium are represented by a non-negative function – the *cross section* – which takes into account all the absorption, emission or scattering phenomena.

The linear Boltzmann equation is widely used in reactor physics and radiation hydrodynamics and many textbooks are devoted to explain the main properties of the equation (see, for example, [4, 10, 11]).

However, at the mathematical level, the linear Boltzmann equation is not yet completely understood, although many properties are already known and a wide quantity of papers prove the interest in the subject.

In particular, the long-time behaviour of the solution of the linear Boltzmann equation is well known only when the cross sections are bounded from below by a strictly positive constant: in such a situation the solution exponentially decays in time to the unique equilibrium state of the system [16] and an explicit upper bound on the spectral gap has been obtained, by means of the hypocoercivity method, by Mouhot and Neumann in [12].

The aforementioned results have, however, no obvious extension in the case of cross sections vanishing in a portion of the domain. Indeed, in the regions where the cross section is zero nether absorption nor scattering are allowed: the problem is locally reduced to the free transport equation, which does not admit any equilibrium state, unless the initial datum is an absolute constant.

Such a transport problem is said to be degenerate, and the complete characterization of the convergence to equilibrium is still an open problem, even if partial answers have been recently provided.

In particular, Desvillettes and Salvarani studied a special situation, by considering cross sections that vanish at a finite number of points [6], and proved an (at least) polynomial speed of convergence to equilibrium, with explicit rates.

Subsequently, Bernard and Salvarani considered in [1] a situation when the cross section vanishes on a set of non-zero measure and gave a counterexample on the exponential convergence to equilibrium by showing that the L^2 distance to equilibrium cannot decay faster than $t^{-1/2}$ in general.

The same authors succeeded, some time later, in characterizing the condition on the cross sections that allows an exponential time decay to the equilibrium state, by means of a non constructive argument and hence without indicating any quantitative estimate of the spectral gap [2]. Such condition has been called the *geometrical condition*. Physically, a cross section satisfies the geometrical condition if and only if there exists a positive constant T_0 such that, for any point (x, v) of the phase space, the characteristic curve $t \mapsto x + tv$, $t \geq 0$, intersects the support of the cross section before the time instant $t = T_0$. In particular, the geometrical condition ensures the non-existence of infinite channels in which the particles move freely.

The analogous result, for unbounded velocity sets, has subsequently been obtained by Han-Kwan and Léautaud in the presence of a force deriving from a potential [8].

The quantitative estimate of the spectral gap is very hard to obtain in the case of degenerate problems. Up to now, the only result, which allows to obtain an optimal convergence rate for degenerate cross sections, has been obtained in [3] for the two-velocity one-dimensional caricature of the linear Boltzmann equation, also known as the Goldstein-Taylor model [7, 15].

It is therefore natural to investigate from a numerical point of view the long-time behaviour of the degenerate linear Boltzmann equation.

In particular, in this article we will quantify:

(1) the spectral gap for a cross section satisfying the geometrical condition given in [2], and
(2) the exponent of the polynomial convergence rate for degenerate cross sections that do not satisfy the geometrical condition.

The numerical method adopted in the article, whose precise description is given in Section 3, is based on a finite-volume strategy in the phase space.

The choice of the numerical algorithm is very delicate. Indeed, since the theoretical behaviour of the equation is partially unknown and the numerical simulations should suggest a mathematical property of the equation, the

guarantee that the numerical procedure is adequate to the problem is of paramount importance.

In particular, we need a procedure which is exempted from numerical diffusion effects in large time, since we need to capture a long-time relaxation to equilibrium which is not necessarily exponential.

Other numerical strategies are, of course, possible, such as a particle method, in the same spirit as in [5] and [13]. However, since the evaluation of the convergence in large-time requires the computation of an integral in the phase space, a huge number of numerical particles is requested in order to have a reasonable accuracy and the computation would be much heavier in comparison with the finite volume method adopted here.

The structure of the article is the following. In the next section we state the problem and summarise the known features of the model. Then, in Section 3 we describe the numerical algorithm and, in Section 4, we show and analyse our numerical simulations. Finally, in a short Appendix, we will give some details about the accuracy of the quadrature rule.

2. The state-of-the-art on the degenerate linear Boltzmann equation

Let $f := f(t, x, v)$ be the solution of the linear Boltzmann equation with isotropic scattering in a periodic box, that is

$$(2.1) \quad \begin{cases} \dfrac{\partial f}{\partial t} + v \cdot \nabla_x f = \sigma(x)\,(\bar{f} - f), & (t, x, v) \in \mathbb{R}_+ \times \mathbb{T}^d \times V \\[2mm] f(0, x, v) = f^0(x, v) & (x, v) \in \mathbb{T}^d \times V, \end{cases}$$

where $\mathbb{T}^d := \mathbb{R}^d/\mathbb{Z}^d$, $(d \in \mathbb{N}, d \geq 2)$. The unknown f represents the density of point particles (usually neutrons or photons) which at time $t \in \mathbb{R}^+$ and point $x \in \mathbb{T}^d$ move at speed $v \in V$.

Here V can denote either the unit sphere in $\mathbb{R}^d$ (when dealing with a monokinetic gas) or the spherical shell individuated by the two radii $0 < v_m < v_M$: that is $V = \mathbb{S}^{d-1}$ or $V = \{v \in \mathbb{R}^d : v_m \leq |v| \leq v_M\}$.

Moreover,

$$\bar{f}(t, x) = \frac{1}{|V|} \int_V f(t, x, v)\, dv,$$

where $|V|$ is the total measure of V.

In what concerns the initial conditions, we assume that $f^0 \in L^\infty(\mathbb{T}^d \times V)$ and that $f^0 \geq 0$ for a.e. $(x, v) \in \mathbb{T}^d \times V$.

The nonnegative function $\sigma(x)$ designates the cross section. We will always suppose that

(1) $\sigma \in L^\infty(\mathbb{T}^d)$ and $\sigma(x) \geq 0$ for a.e. $x \in \mathbb{T}^d$;
(2) $\|\sigma\|_{L^1(\mathbb{T}^d)} > 0$.

It is easy to prove that constants are steady solutions of Equation (2.1) and that

$$f_\infty = \frac{1}{|V|} \int_{\mathbb{T}^d \times V} f^0(x, v)\, dx dv$$

is the unique constant solution with the same total mass (i.e. particle number) as the initial data.

In what follows, we will often use a special family of cross sections, which are well suitable when studying degenerate cross section. For this reason, for all $r \in (0, 1/2)$ we introduce the periodic open set

$$Z_r = \{x \in \mathbb{R}^d \,:\, \mathrm{dist}(x, \mathbb{Z}^d) > r\}$$

together with the associated fundamental domain $Y_r = Z_r / \mathbb{Z}^d$.

In [1] the exponential convergence in time to equilibrium – for general cross sections satisfying the previous assumptions – has been excluded, as stated in the following theorem:

Theorem 2.1. (Bernard, Salvarani). *Let $V = \mathbb{S}^{d-1}$. For all $r \in (0, 1/2)$, there exists an initial condition $f^0 \in L^\infty(\mathbb{T}^d \times V)$ satisfying $f^0(x, v) \geq 0$ for a.e. $(x, v) \in \mathbb{T}^d \times V$ and such that, for each cross section $\sigma \in L^\infty(\mathbb{T}^d)$ satisfying $\sigma(x) \geq 0$ for a.e. $x \in \mathbb{T}^d$ and $\sigma(x) = 0$ for a.e. $x \in Y_r$, the solution f of the Cauchy problem (2.1) satisfies*

$$E(t) := \|f - f_\infty\|_{L^2(\mathbb{T}^d \times V)} \geq \frac{C}{\sqrt{t}}$$

for each $t > r^{1-d}$, where C is a positive constant.

However, there exists a class of cross sections that have a nicer behaviour in what concerns the relaxation to equilibrium.

The properties satisfied by σ that lead to an exponential convergence rate in time to the stationary solution have been individuated by Bernard and Salvarani in [2].

Definition 2.2. *The cross section $\sigma \equiv \sigma(x)$ is said to verify the geometrical condition if and only if there exist T_0 and $C > 0$ such that*

$$(2.2) \qquad \int_0^{T_0} \sigma\left(\phi_{x,v}(s)\right) ds \geq C \ a.e. \ in \ (x, v) \in \mathbb{T}^d \times V,$$

where $\phi_{x,v}$ designates the linear flow starting at $x \in \mathbb{T}^d$ in the direction $-v \in V$:

$$\phi_{x,v} : t \mapsto x - tv.$$

The main result of [2] is the proof that the exponential convergence is a direct consequence of the geometrical condition:

Theorem 2.3. (Bernard, Salvarani). *Let $\sigma \in L^\infty\left(\mathbb{T}^d\right)$ be a non-negative cross section satisfying the geometrical condition (2.2). Then there exist two constants $M > 0$ and $\alpha > 0$ such that the solution f of the Cauchy problem (2.1) satisfies the inequality*

$$(2.3) \qquad \left\| f - \int_{\mathbb{T}^d \times V} f^0(x, v)\, dx dv \right\|_{L^1\left(\mathbb{T}^d \times V\right)} \leq M e^{-\alpha t} \left\| f^0 \right\|_{L^1\left(\mathbb{T}^d \times V\right)}$$

for all $t \in \mathbb{R}_+$. Conversely, if the solution of the Cauchy problem (2.1) converges uniformly in L^1 to its equilibrium state at an exponential rate (i.e. satisfies (2.3)), then σ must satisfy the geometrical condition (2.2).

3. The numerical discretization

In what follows, we will restrict ourselves to the $2D$ (in space) monokinetic case, i.e. we will suppose that $x \in \mathbb{T}^2 = (0,1)^2$, $v \in \mathbb{S}^1$ and that f satisfies the equation

(3.1)
$$\frac{\partial f}{\partial t} + v \cdot \nabla_x f = \sigma(x) \left[\int_0^{2\pi} f(t, x, \omega) \frac{d\omega}{2\pi} - f \right] \quad x \in \mathbb{T}^2, \ \omega \in [0, 2\pi), \ t > 0,$$

where $v = v(\omega) = (\cos \omega, \sin \omega)$. Initially, the distribution is known: $f = f^0 \in L^\infty(\mathbb{T}^2 \times \mathbb{S}^1)$, periodic in the phase space, with $\|f^0\|_{L^1(\mathbb{T}^2 \times \mathbb{S}^1)} = 1$. We will assume periodic boundary conditions for both spatial and angle variables. Denoting by

$$\rho(x, t) = \frac{1}{2\pi} \int_0^{2\pi} f(t, x, \omega) \, d\omega$$

the marginal probability density function for the space variable, the following conservative equation holds

$$\partial_t \rho + \nabla \cdot \left[\frac{1}{2\pi} \int_0^{2\pi} f(t, x, \omega) v(\omega) \, d\omega \right] = 0.$$

Then it is expected that $\|f(t, \cdot, \cdot)\|_{L^1(\mathbb{T}^2 \times \mathbb{S}^1)} = 1$ for all time t.

We first consider the time discretization. Let us denote $f^n(x, \omega)$ an approximate value of $f(t = t^n, x, \omega)$. Consider a constant time step $\Delta t > 0$ and let $t^{n+1} = t^n + \Delta t$. For time advance, it is convenient to consider here a fractional step approach, by handling transport and scattering separately and sequentially. We shall use the well-known second-order Strang splitting scheme.

Let $\mathscr{R}^{\Delta t}$ denote the operator such that the distribution $f = \mathscr{R}^{\Delta t} f^0$ is the exact solution at time Δt of the pure scattering problem with f^0 as initial data:

(3.2) $\quad \dfrac{\partial f}{\partial t} = \sigma(x) \left[\int_0^{2\pi} f(t, x, \omega) \dfrac{d\omega}{2\pi} - f \right] \quad x \in \mathbb{T}^2, \ \omega \in [0, 2\pi), \ t > 0,$

(3.3) $\quad f(t = 0, x, \omega) = f^0(x, \omega).$

Let $\mathscr{T}^{\Delta t}$ the transport operator over a time step Δt:

$$\mathscr{T}^{\Delta t} f^0(x, \omega) = f^0(x + v(\omega) \Delta t, \omega).$$

Then a second order accurate solution (in Δt) of the solution of the whole scattering problem is given by the Strang splitting approximation:

(3.4) $$f(\Delta t, \cdot) \approx \mathscr{R}^{\Delta t/2} \ \mathscr{T}^{\Delta t} \ \mathscr{R}^{\Delta t/2} f^0.$$

This leads to the discrete time advance scheme

(3.5) $$f^{n+1} = \mathscr{R}^{\Delta t/2} \ \mathscr{T}^{\Delta t} \ \mathscr{R}^{\Delta t/2} f^n.$$

For recovering the full discretization, we now have to approximate both transport and scattering operators.

In what follows, we will need working with the components of the vectors x and v. We will hence denote $x = (\bar{x}, \bar{y}) \in \mathbb{T}^2$.

Let
$$i \in \{1, \ldots, I\}, \quad j \in \{1, \ldots, I\}, \quad k \in \{1, \ldots, K\}.$$
We will denote by f_{ijk}^n (or $f_{i,j,k}^n$ for readability purposes) an approximate value of $f(t^n, \bar{x}_i, \bar{y}_j, \omega_k)$ considering a Cartesian spatial grid of constant mesh size $h = 1/I$,
$$\bar{x}_i = \left(i - \frac{1}{2}\right)h, \quad \bar{y}_j = \left(j - \frac{1}{2}\right)h, \quad \omega_k = \frac{2\pi}{K}\left(k - \frac{1}{2}\right).$$
We will also use the notations
$$x_{ij} = (\bar{x}_i, \bar{y}_j), \quad \sigma_{ij} = \sigma(x_{ij}), \quad v_k = v(\omega_k) = (\cos(\omega_k), \sin(\omega_k)).$$

3.1. **Scattering step.** For the full discretization of the pure scattering problem, we have to consider a quadrature formula of the integral term and a second order accurate time advance scheme. It has been shown by Kurganov and Rauch [9] that the trapezoidal rule actually provides spectral accuracy. For the interested reader, in the short Appendix A we recall some of the results proved in [9]. The trapezoidal rule on periodic functions gives

$$(3.6) \qquad \frac{1}{2\pi} \int_0^{2\pi} f(t^n, x_{ij}, \omega) \, d\omega \approx \frac{1}{K} \sum_{k=1}^{K} f(t^n, x_{ij}, \omega_k).$$

This quadrature formula is then used into the second order predictor-corrector time advance scheme:

$$(3.7) \qquad f_{ijk}^{n+1/2,\star} = f_{ijk}^n + \frac{\Delta t}{4}\sigma_{ij}\left[\frac{1}{K}\sum_{\ell=1}^{K} f_{i,j,\ell}^n - f_{ijk}^n\right],$$

$$(3.8) \qquad f_{ijk}^{n+1/2} = f_{ijk}^n + \frac{\Delta t}{2}\sigma_{ij}\left[\frac{1}{K}\sum_{\ell=1}^{K} f_{i,j,\ell}^{n+1/2,\star} - f_{ijk}^{n+1/2,\star}\right].$$

We naturally fulfil the conservation property at the discrete level

$$(3.9) \qquad \sum_{k=1}^{K} f_{ijk}^{n+1/2} = \sum_{k=1}^{K} f_{ijk}^n.$$

3.2. **Transport step.** We propose a simple second order accurate (in both space and time) conservative Eulerian solver for the K pure transport problems

$$(3.10) \qquad \partial_t f_k + v_k \cdot \nabla_x f_k = 0,$$

$$(3.11) \qquad f_k(t = 0) = f_k^0.$$

We have to take care of possible spurious oscillations for low-regularity solutions adding numerical viscosity and, at the same time, to avoid artificial diffusive effects in the large-time behaviour. We propose to use a conservative finite-volume scheme combining a Lax-Wendroff second-order viscosity term (for second-order time accuracy) and an artificial viscosity term involving slope reconstructions and slope limiters.

The conservative scheme reads

$$f_{ijk}^{n+1} = f_{ijk}^n - \frac{\Delta t}{h}\left[\Phi_{i+1/2,j,k}^{n+1/2} - \Phi_{i-1/2,j,k}^{n+1/2}\right] - \frac{\Delta t}{h}\left[\Phi_{i,j+1/2,k}^{n+1/2} - \Phi_{i,j-1/2,k}^{n+1/2}\right]$$

with convective fluxes $\Phi_{i+1/2,j,k}^{n+1/2}$ and $\Phi_{i,j+1/2,k}^{n+1/2}$ in the $\bar{x}$ and $\bar{y}$ directions, respectively. The numerical flux in the $\bar{x}$-direction is given by
(3.12)

$$\Phi_{i+1/2,j,k}^{n+1/2} = \frac{f_{i,j,k}^n + f_{i+1,j,k}^n}{2}\cos(\omega_k)$$

$$-\frac{1}{2}\frac{\Delta t}{h}|\cos(\omega_k)|(f_{i+1,j,k}^n - f_{i,j,k}^n) - \frac{1}{2}|\cos(\omega_k)|(\tilde{f}_{i+1,j,k}^{-,n} - \tilde{f}_{i,j,k}^{+,n})$$

with the interpolated states at the $\bar{x}$-interfaces

$$(3.13)\qquad \tilde{f}_{i,j,k}^{\pm,n} = f_{i,j,k}^n \pm \frac{1}{2}\operatorname{minmod}(f_{i+1,j,k}^n - f_{i,j,k}^n, f_{i,j,k}^n - f_{i-1,j,k}^n),$$

where the last term in the right-hand-side of (3.13) is the classical *minmod* slope limiter function:

$$\operatorname{minmod}(a,b) = \operatorname{sign}(a)\,\mathbb{1}_{(ab>0)}\,\min(|a|,|b|).$$

The numerical fluxes in the $\bar{y}$ direction are constructed in the same way.

Because of its explicit feature, the finite-volume scheme is conditionally stable, subject to a Courant-Friedrichs-Lewy (CFL) condition. Since the discrete velocities v_k are all unit vectors, we will use the time step corresponding to CFL number "one-half"

$$(3.14)\qquad\qquad\qquad \frac{\Delta t}{h} = \frac{1}{2}$$

setting the time step value. By construction, the whole numerical scheme is second-order accurate on both space and time. The quadrature formula used for the angle integrals into the scattering term has the spectral accuracy (see appendix A) and so it will be accurate for sufficiently smooth solutions.

3.3. Remarks on the free transport. It is well known that the numerical approximation of free transport phenomena in periodic domains is very delicate when dealing with a finite discretization on the velocity set [14]. Indeed, non physical plateaux of order of $t\Delta v$ can appear in the solution and influence the numerical result.

It is apparent that a correct treatment of the free transport is crucial in our case, since the lack of exponential convergence to equilibrium is a consequence of the existence of infinite channels in which only the free transport is allowed, as explained in the Introduction.

In particular, if the discrete velocity set would not include the directions of the infinite free channels, the discretization would artificially remove the degeneracy of the problem: after a possibly large but finite time interval, all the numerical optical paths would intersect the scattering region, and hence an exponential-like convergence could be observed.

On the other hand, if the numerical set of velocities includes the direction of an infinite channel, denoted as $\bar{\omega}_k$, the numerical procedure induces an overpopulation of such directions, since all the optical paths whose directions belong to the interval $[\bar{\omega}_k - \pi/K, \bar{\omega}_k + \pi/K]$ will be identified with the
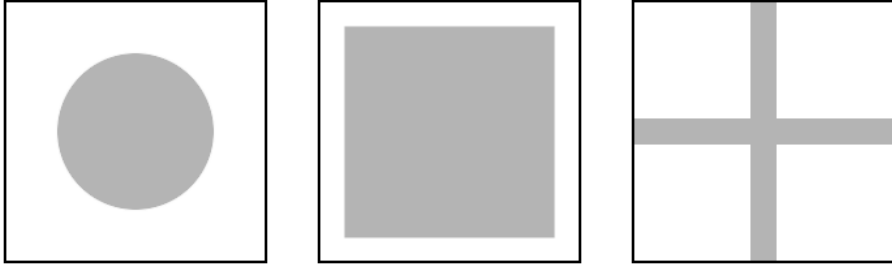
FIGURE 1. Cross sections σ_1 (left), σ_2 (centre) and σ_3 (right). The white region shows the points of $\mathbb{T}^2$ where the cross sections vanish.

direction of the infinite channel itself. In this case, the numerical simulations will underestimate the decay, especially in large time.

However, the method described here is sufficiently accurate for our purposes, as shown in the next Section.

4. NUMERICAL EVIDENCE OF LARGE-TIME BEHAVIOUR

Consider the problem on the unit spatial square domain $\mathbb{T}^2 = [0,1]^2$, with periodic spatial boundary conditions and with initial condition f^0 such that $\|f^0\|_{L^1(\mathbb{T}^2 \times \mathbb{S}^1)} = 1$. By the mass conservation, we have that the steady state is $f_\infty = 1$. We will evaluate the time evolution for the squared L^2-norm of the deviation to the steady state f_∞, i.e. the time evolution of the quantity

$$(4.1) \qquad E^2(t) := \|f(t, \cdot, \cdot) - f_\infty\|^2_{L^2(\mathbb{T}^2 \times \mathbb{S}^1)},$$

for different types of cross sections.

For the numerical discretization, unless otherwise specified, we consider a h-uniform Cartesian spatial grid composed of 256×256 points. For the angle variable discretization, we also use a uniform grid $\omega_k = 2\pi(k-1/2)/K$, $k = 1, \dots, K$ with $K = 256$. So this discrete problem is composed of $256^3 = 16,777,216$ grid points.

We also show two numerical experiments with different discretizations of the domain, in order to show how the grid influences the numerical results.

We use a fixed time step, as prescribed by (3.14). In all simulations, the computational time window is $t \in [0, T]$, with $T = 12$.

4.1. **A circular degenerate cross section.** We consider here the specific cross section $\sigma : \mathbb{T}^2 \to \mathbb{R}$ defined, in the fundamental domain $\mathbb{T}^2$, by

$$\sigma = \sigma_1 := 20 \times \mathbb{1}_{\mathbb{T}^2 \setminus Y_{1/4}},$$

(see Figure 1, left), and the initial condition is

$$f^0(x, \omega) = \frac{1}{2\pi} \frac{1 - \mathbb{1}_{\mathbb{T}^2 \setminus Y_{1/4}}}{\|1 - \mathbb{1}_{\mathbb{T}^2 \setminus Y_{1/4}}\|_{L^1}} \quad \forall x \in \mathbb{T}^2, \omega \in [0, 2\pi].$$

By construction, $\|f^0\|_{L^1(\mathbb{T}^2 \times \mathbb{S}^1)} = 1$. Note that the cross section (which does not satisfy the geometrical condition) and the initial condition are, up to a normalization factor, the same used for proving Theorem 2.1 in [1]. Hence,

we can compare the numerical simulations to a theoretical result that gives an upper bound on the L^2-distance between the solution at time t and the equilibrium.
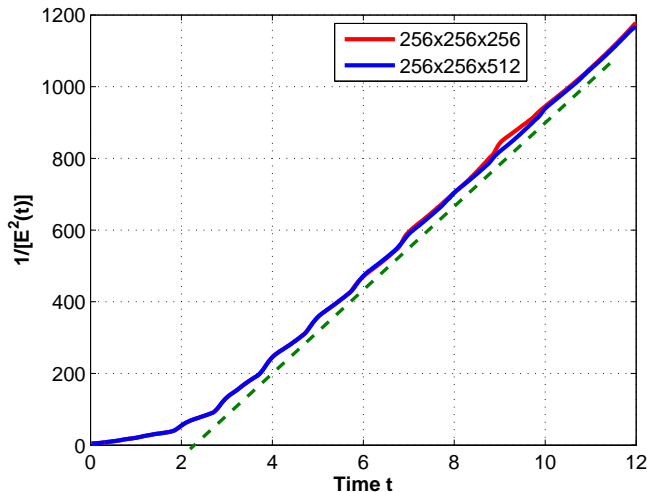
FIGURE 2. Time evolution of $1/E^2(t)$, with cross section σ_1 with two different discertizations in velocity. The behaviour is linear in time.

Our numerical experiments show that $1/E^2(t)$ increases in time like t faithfully. At first instants, between the initial time and roughly time $t = 3$, the discrepancy decreases at a lower rate, then the linear fit becomes almost perfect after time $t = 3$. It is observed on Figure 2 that

$$E^2(t) \simeq \frac{C}{t}, \quad t \geq 3$$

for a constant $C > 0$.

We note moreover that the simulation with $256 \times 256 \times 512$ grid points and the simulation with 256^3 grid points give very similar result.

Finally, for information purposes, we also plot on Figures 3 and 4 the contour of the discrete marginal distribution

$$x \mapsto \int_0^{2\pi} f(t^n, x, \omega) \, d\omega.$$

at $t^0 = 0$ and at different discrete instants t^n respectively.

We remark that the discrete solution does not lead to strong changes of gradient and that the slope limiter of the transport solver does not generate first-order numerical diffusion and $O(h)$ errors.

Our numerical simulations hence suggest that the theoretical large-time lower bound behaviour on E of order $t^{-1/2}$ is the exact decay rate.

4.2. **A squared degenerate cross section.** Let $(\bar{x}, \bar{y}) \in \mathbb{T}^2$. We consider here the specific cross section $\sigma \ : \ \mathbb{T}^2 \to \mathbb{R}$ defined, in the fundamental
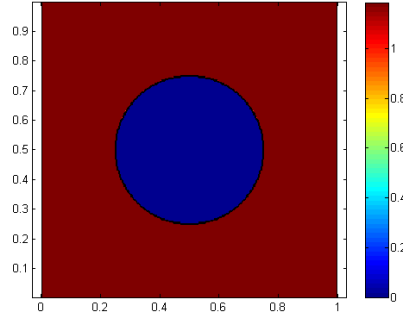
FIGURE 3. Contour of the marginal spatial distribution (with cross section σ_1): initial condition.

domain $\mathbb{T}^2$, by

$$\sigma = \sigma_2 := \left\{ \begin{array}{ll} 20 & 0.1 \leq \bar{x} \leq 0.9 \text{ and } 0.1 \leq \bar{y} \leq 0.9 \\ 0 & \text{otherwise} \end{array} \right.$$

(see Figure 1, centre). This cross section does not satisfy either the geometrical condition, hence we cannot expect, by Theorem 2.3, an exponential convergence to equilibrium. Moreover, it does not exist any ball of radius $r < 1/2$ such that the support of σ_2 is embedded into the ball. Hence, the estimate of Theorem 2.1 – based on the geometrical properties of a circular support of the scattering region – cannot be applied here.

The initial condition here is given by

$$f^0(x, \omega) = \frac{1}{2\pi} \frac{1 - \mathbb{1}_{\{(\bar{x}, \bar{y}) \in \mathbb{T}^2, \ 0.1 \leq \bar{x} \leq 0.9 \text{ and } 0.1 \leq \bar{y} \leq 0.9\}}}{\|1 - \mathbb{1}_{\{(\bar{x}, \bar{y}) \in \mathbb{T}^2, \ 0.1 \leq \bar{x} \leq 0.9 \text{ and } 0.1 \leq \bar{y} \leq 0.9\}}\|_{L^1}},$$

$x \in \mathbb{T}^2$, $\omega \in [0, 2\pi]$. By construction $\|f^0\|_{L^1(\mathbb{T}^2 \times \mathbb{S}^1)} = 1$.

This numerical experiment is the most delicate one, since the region of degeneracy covers a small portion of the domain and, at the same time, it includes two infinite channels. We can hence expect that coarse grids generate bad results.

In Figure 5 we have superposed three plots. The first one has been obtained by using an uniform grid with 128^3 points in the phase space. This numerical simulation is very poor, especially after $t = 5$.

The second plot refers to an uniform grid with 256^3 points in the phase space, such that the directions of the infinite channels coincide with some discretized velocity directions. It shows that $1/E^2(t)$ increases in time like t up to $t = 10$, and then the convergence speed to equilibrium slightly degrades for $10 \leq t \leq 12$.

In the third numerical experiment, obtained by working in a phase-space grid with $256 \times 256 \times 512$ points, the quantity $1/E^2(t)$ increases in time like t up to $t = 12$, without showing any degradation of the trend to equilibrium.

The differences between the two last experiments can be explained in terms of the sensitivity of the procedure with respect to the discretization of the velocities whose directions are close to the direction of the infinite
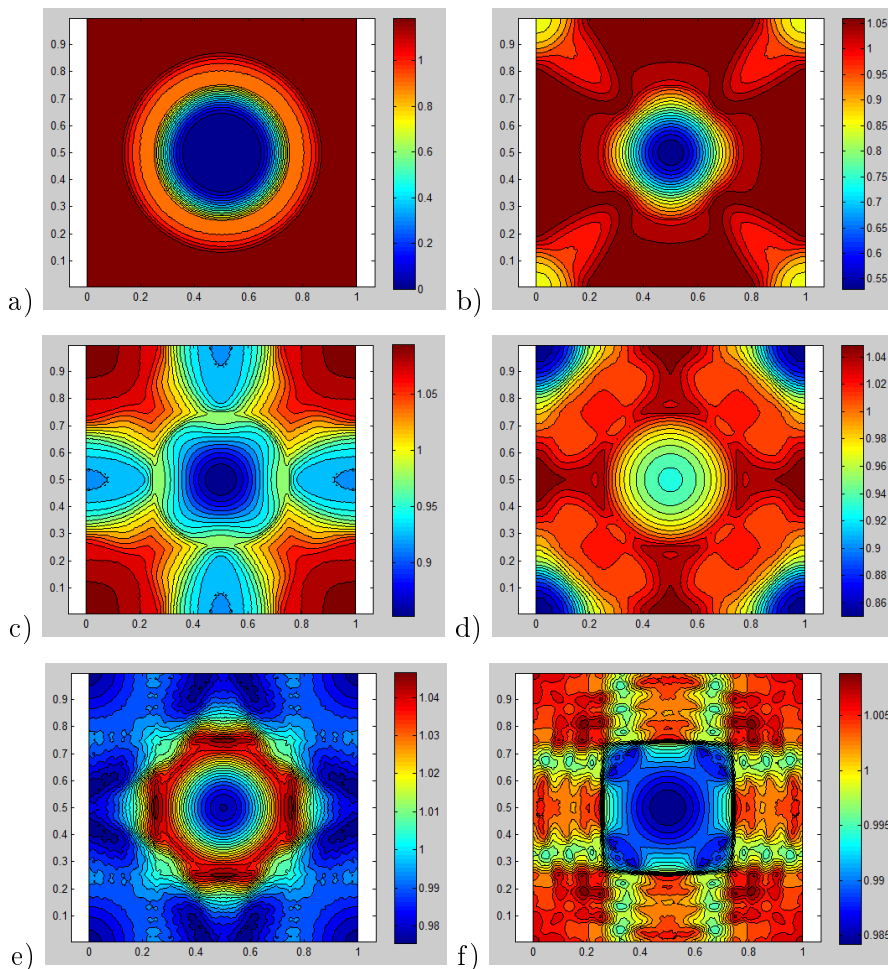
FIGURE 4. Contours of the marginal spatial distribution, with cross section σ_1, for six different instants: a) $t = 0.08$, b) $t = 0.62$, c) $t = 1.00$, d) $t = 1.50$, e) $t = 1.80$ and f) $t = 3.50$.

channels, as discussed in Subsection 3.3. The overall qualitative behaviour of the plots provides a numerical evidence of the convergence of the method.

4.3. **A degenerate cross section satisfying the geometrical condition.** We finally tested the situation of a cross section that satisfies the geometrical condition. In this case, Theorem 2.3 gives a result of convergence to equilibrium of exponential type with respect to the L^1-norm.

Let $(\bar{x}, \bar{y}) \in \mathbb{T}^2$. We consider the cross sections $\sigma_3 : \mathbb{T}^2 \to \mathbb{R}$ defined as

$$(4.2) \qquad \sigma = \sigma_3 := \begin{cases} 20 & 0.45 \le \bar{x} \le 0.55, \text{ or } 0.45 \le \bar{y} \le 0.55 \\ 0 & \text{otherwise} \end{cases}$$

(see Figure 1, right).

The initial condition here is given by

$$f^0(x, \omega) = \frac{1}{2\pi} \, \frac{1 - \mathbb{1}_{\{(\bar{x}, \bar{y}) \in \mathbb{T}^2, \, 0.45 \le \bar{x} \le 0.55 \text{ or } 0.45 \le \bar{y} \le 0.55\}}}{\left\| 1 - \mathbb{1}_{\{(\bar{x}, \bar{y}) \in \mathbb{T}^2, \, 0.45 \le \bar{x} \le 0.55 \text{ or } 0.45 \le \bar{y} \le 0.55\}} \right\|_{L^1}},$$
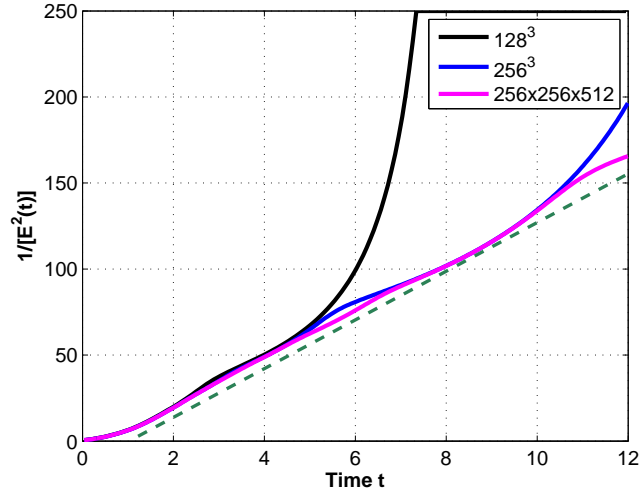
FIGURE 5. Time history of $1/E^2(t)$, with cross section σ_2 and with three different discretizations of the phase space.

$x \in \mathbb{T}^2$, $\omega \in [0, 2\pi]$. By construction $\|f^0\|_{L^1(\mathbb{T}^2 \times \mathbb{S}^1)} = 1$.

The numerical simulation agrees with the theoretical result, and an exponential convergence in L^1-norm has been numerically observed (see Figure 6).
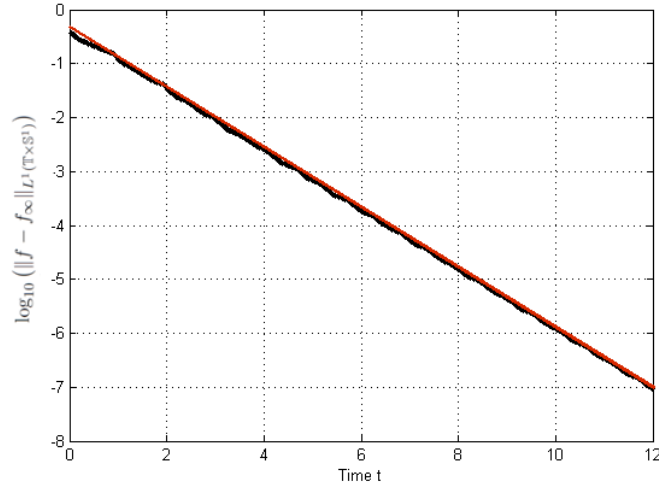
FIGURE 6. Time evolution of $\log_{10}\left(\|f - f_\infty\|_{L^1(\mathbb{T} \times \mathbb{S}^1)}\right)$ with cross section σ_3. The behaviour is exponential in time.

We finally show, in Figure 7, the time decay of E. Indeed, we are interested in comparing, with respect to the same metrics, the different time decays obtained with different cross sections. Again in this case, we obtain exponential convergence to equilibrium.

This result gives a numerical confirmation of the sufficiency of the geometrical condition for obtaining an exponential decay to equilibrium.
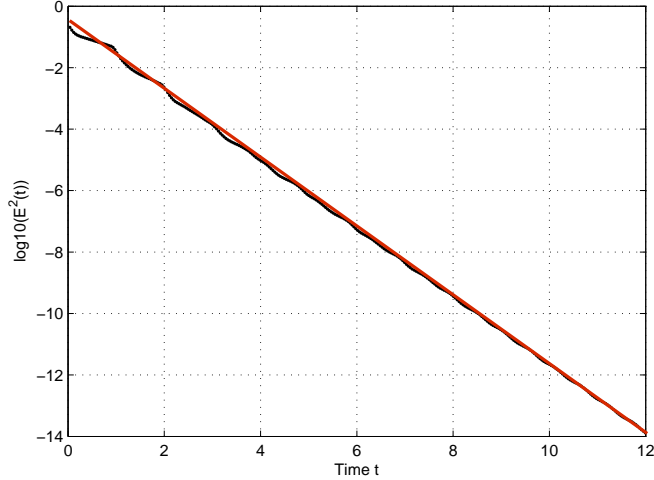
FIGURE 7. Time evolution of $2\log_{10}(E(t))$ with cross section σ_3. The behaviour of $E(t)$ is exponential in time.

APPENDIX A. QUADRATURE FORMULA FOR PERIODIC FUNCTIONS

We give here some comments about the choice of the quadrature formula for the angle variable integration and we mainly refer to a note by Kurganov and Rauch [9]. Denote by $W_{per}^{r,p}$ the Banach space of periodic functions on $\mathbb{R}$ whose derivatives up to order r belongs to $L_{per}^p(\mathbb{R})$. The trapezoidal rule

$$\int_0^{2\pi} f(\omega)\,d\omega \approx T_K(f) := \frac{2\pi}{K}\sum_{k=1}^{K} f(\omega_k), \quad \omega_k = \frac{2\pi}{K}\left(k - \frac{1}{2}\right), \quad k = 1,\ldots,K,$$

appears to be relevant because of the periodicity and the invariance by translation. The quadrature error is equal to

$$E_N(f) = T_N(f) - \int_0^{2\pi} f(\omega)\,d\omega.$$

Since f is periodic in ω, it can be written as a Fourier series:

$$f(x) = \sum_{n\in\mathbb{Z}} c_n e^{in\omega}, \quad c_n = \frac{1}{2\pi}\int_0^{2\pi} f(\omega)e^{-in\omega}\,d\omega.$$

Let $\mathcal{P}(m)$ be the set of all trigonometric polynomials of degree at most m. Summing finite geometric series shows that $T_K(e^{in\omega}) = 0$ for $0 < |n| < K$: hence T_K is an exact quadrature formula for trigonometric polynomials of degree $K - 1$. For any $P \in \mathcal{P}(K - 1)$, we then have

$$E_K(f) = E_K(f - P) = T_N(f - P) - \int_0^{2\pi} (f(\omega) - P(\omega))\,d\omega$$

and we get the estimate

$$|E_K(f)| \leq 4\pi \inf_{P \in \mathcal{P}(K-1)} \|f - P\|_{L^\infty}.$$

The trapezoidal rule thus provides spectral accuracy because of the rapid decay of the Fourier coefficients for infinitely smooth functions f. Kurganov and Rauch [9] were able to show that, for $f \in W_{per}^{r,1}$ and $1 < r$, the error of the trapezoidal quadrature rule satisfies

$$|E_K(f)| \leq \frac{C}{K^r} \|f^{(r)}\|_{L^1([0,2\pi])}, \quad C := 2 \sum_{k=1}^{\infty} \frac{1}{k^r}.$$

REFERENCES

[1] Étienne Bernard and Francesco Salvarani. On the convergence to equilibrium for degenerate transport problems. *Arch. Ration. Mech. Anal.*, 208(3):977–984, 2013.

[2] Étienne Bernard and Francesco Salvarani. On the exponential decay to equilibrium of the degenerate linear Boltzmann equation. *J. Funct. Anal.*, 265(9):1934–1954, 2013.

[3] Étienne Bernard and Francesco Salvarani. Optimal Estimate of the Spectral Gap for the Degenerate Goldstein-Taylor Model. *J. Stat. Phys.*, 153(2):363–375, 2013.

[4] Kenneth M. Case and Paul F. Zweifel. *Linear transport theory*. Addison-Wesley Publishing Co., Reading, Mass.-London-Don Mills, Ont., 1967.

[5] Florian De Vuyst and Francesco Salvarani. Gpu-accelerated numerical simulations of the knudsen gas on time-dependent domains. *Comput. Phys. Comm.*, 184(3):532–536, 2013.

[6] Laurent Desvillettes and Francesco Salvarani. Asymptotic behavior of degenerate linear transport equations. *Bull. Sci. Math.*, 133(8):848–858, 2009.

[7] S. Goldstein. On diffusion by discontinuous movements, and on the telegraph equation. *Quart. J. Mech. Appl. Math.*, 4:129–156, 1951.

[8] Daniel Han-Kwan and Matthieu Léautaud. Geometric analysis of the linear boltzmann equation i. trend to equilibrium, 2014.

[9] Alexander Kurganov and Jeffrey Rauch. The order of accuracy of quadrature formulae for periodic functions. In *Advances in phase space analysis of partial differential equations*, volume 78 of *Progr. Nonlinear Differential Equations Appl.*, pages 155–159. Birkhäuser Boston Inc., Boston, MA, 2009.

[10] E. E. Lewis and W. F. Miller. *Computational methods of neutron transport*. John Wiley and Sons, Inc.,New York, NY, 1984.

[11] M. Mokhtar-Kharroubi. *Mathematical topics in neutron transport theory*, volume 46 of *Series on Advances in Mathematics for Applied Sciences*. World Scientific Publishing Co. Inc., River Edge, NJ, 1997. New aspects, With a chapter by M. Choulli and P. Stefanov.

[12] Clément Mouhot and Lukas Neumann. Quantitative perturbative study of convergence to equilibrium for collisional kinetic models in the torus. *Nonlinearity*, 19(4):969–998, 2006.

[13] Francesco Salvarani. On the linear boltzmann equation in evolutionary domains with absorbing boundary. *J. Phys. A: Math. Theor.*, 46:355501, 2013.

[14] Brull Stéphane and Luc Mieussens. Local discrete velocity grids for deterministic rarefied flow simulations, 2013.

[15] G. I. Taylor. Diffusion by Continuous Movements. *Proc. London Math. Soc.*, S2-20(1):196.

[16] Seiji Ukai, Nelly Point, and Hamid Ghidouche. Sur la solution globale du problème mixte de l'équation de Boltzmann nonlinéaire. *J. Math. Pures Appl. (9)*, 57(3):203–229, 1978.

F.D.V: Centre de Mathématiques et de leurs Applications, CMLA UMR 8536, École Normale Supérieure de Cachan, 61 avenue du Président Wilson, 94235 Cachan France
E-mail address: `devuyst@cmla.ens-cachan.fr`

F.S.: Dipartimento di Matematica F. Casorati, Università degli Studi di Pavia, Via Ferrata 1, I-27100 Pavia, Italy
E-mail address: `francesco.salvarani@unipv.it`